Published in final edited form as:
J Control Release. 2012 September 10; 162(2): 355–363. doi:10.1016/j.jconrel.2012.07.025.

Cellular and vascular effects of the photodynamic agent temocene are modulated by the delivery vehicle

María García-Díaz[1,2,3], **Masayoshi Kawakubo**[2,4,5], **Pawel Mroz**[2,4], **M. Lluïsa Sagristà**[3], **Margarita Mora**[3], **Santi Nonell**[1,*], and **Michael R. Hamblin**[2,4,6,*]

[1]Molecular Engineering Group, IQS School of Engineering, Universitat Ramon Llull, Barcelona, Spain

[2]Wellman Center for Photomedicine, Massachusetts General Hospital, Boston, MA 02114

[3]Departament de Bioquimica i Biologia molecular, Universitat de Barcelona, Barcelona, Spain

[4]Department of Dermatology, Harvard Medical School, Boston, MA 02115

[5]Department of Surgery, School of Medicine, Keio University, Tokyo, Japan

[6]Harvard-MIT Division of Health Sciences and Technology, Cambridge, MA 02139

Abstract

The effects of the drug delivery system on the PDT activity, localization, and tumor accumulation of the novel photosensitizer temocene (the porphycene analogue of temoporfin or *m*-tetrahydroxyphenyl chlorin) were investigated against the P815 tumor, both *in vitro* and in DBA/2 tumor bearing mice. Temocene was administered either free (dissolved in PEG_{400}/EtOH mixture), or encapsulated in Cremophor EL micelles or in DPPC/DMPG liposomes, chosen as model delivery vehicles. The maximum cell accumulation and photodynamic activity *in vitro* was achieved with the free photosensitizer, while temocene in Cremophor micelles hardly entered the cells. Notwithstanding, the micellar formulation showed the best *in vivo* response when used in a vascular regimen (short drug light interval), whereas liposomes were found to be an efficient drug delivery system for a tumor cell targeting strategy (long drug-light interval). PEG/EtOH formulation was discarded for further *in vivo* experiments as it provoked lethal toxic effects caused by photosensitizer aggregation. These results demonstrate that drug delivery systems modulate the vascular and cellular outcomes of photodynamic treatments with temocene.

Keywords

Photodynamic therapy; porphycene; temocene; liposome; micelle; localization; vascular targeting; cellular targeting

*Corresponding authors: Santi Nonell - Mailing address: Grup d'Enginyeria Molecular, Institut Quimic de Sarrià, Universitat Ramon Llull, Via Augusta 390, 08017 Barcelona, Spain. santi.nonell@iqs.url.edu and Michael R. Hamblin – Mailing address: Wellman Center for Photomedicine, Massachusetts General Hospital, 40 Blossom St., Boston, MA 02114, USA. hamblin@helix.mgh.harvard.edu. Phone 617-726-6182; Fax 617-726-8566.

Introduction

Photodynamic therapy (PDT) is a tumor treatment modality that uses light, oxygen and a photosensitizer (PS) for the destruction of targeted tissues [1,2]. These components are individually non-toxic, but together they generate cytotoxic reactive oxygen species (ROS) leading to cellular damage [3]. The PS absorbs a photon to form excited states that can undergo electron transfer (type I reaction) generating superoxide, hydrogen peroxide, and hydroxyl radicals; or they can instead transfer energy to molecular oxygen to produce highly cytotoxic singlet oxygen (type II reaction).

There are three main mechanisms that operate to allow PDT to destroy tumors: 1) direct cellular killing by necrosis and/or apoptosis [4–6], 2) tumor-associated vascular damage leading to thrombosis and hemorrhage that subsequently cause tumor hypoxia [7–9], and 3) activation of antitumor immune response contributing to tumor destruction even in distant locations [10–12]. It is generally accepted that all three mechanisms are necessary for the optimal tumor damage. The relative contribution of these pathways depends upon the PS used, the tissue being treated, and treatment conditions. For a particular tissue and PS, the targeting strategy can be modulated by illumination at a short or long interval after drug administration, maximizing vascular or cellular targeting, respectively. The PS is predominantly retained in the tumor vasculature initially after i.v. injection, and light delivery within minutes after administration damages the tumor vasculature [13]. This mechanism has received considerably attention in recent years due to the successful clinical implementation of PDT in age-related macular degeneration treatment with verteporfin [14] and prostate cancer treatment with Pd-bacteriochlorophyll derivatives TOOKAD and WST11 [15–17]. Conventional cancer cell targeting approaches allow the PS to freely diffuse out into the tissue and to accumulate into the tumor cellular compartment. A long drug-to-light interval generates more direct cytotoxic cellular damage. The selectivity of this strategy relies on the preferential drug accumulation in the tumor relative to the surrounding normal tissue.

Thus, pharmacokinetics of the PS plays an important role in effectiveness of both vascular and cellular PDT. Pharmacokinetics and selectivity can be enhanced by nanoparticles as vehicles for PS delivery. Different approaches have been developed to enable selective accumulation of the PS providing an environment where the PS can be administered in monomeric form and without loss or alteration of its activity [18–21]. Indeed lipid and detergent nanostructures (liposomes and micelles) have been extensively used in PDT. To further investigate these questions, we evaluated the influence of different formulations in PDT effectiveness both *in vitro* and *in vivo*. The novel PS temocene [22] was chosen as photoactive molecule in this study.

Temocene is the porphycene analogue to *m*-tetrahydroxyphenyl chlorin, commonly named temoporfin. In a previous work [22], we showed that both the photophysical properties and photodynamic activity *in vitro* suggested that temocene was a good candidate for PDT. These results prompted us to extend our studies to *in vivo* assays, which required the development of an effective drug delivery vehicle. Based on the fact that temoporfin is used clinically either dissolved in a PEG_{400}-EtOH mixture (trade name Foscan®) or formulated in liposomes (Foslip®), we adopted such vehicles for our studies and included additionally Cremophor EL micelles as systems of intermediate complexity.

As mentioned above, the targeting strategy is a critical parameter for the success of PDT. Thus, the effects of drug-to-light interval on tumor regression were also investigated. Formulations were administered intravenously and PDT was performed 15 min (vascular targeting) or 24 h (cellular targeting) after injection. We found that Cremophor EL micelles

using a vascular targeted short drug-to-light interval PDT was the best combination for a successful treatment.

Experimental section

Chemicals

The synthesis, molecular characterization and photophysical properties of temocene (Fig. 1A) have been previously described in detail [22]. For cellular and *in vivo* studies, temocene was dissolved in PEG_{400}/EtOH (3:2) or formulated in micelles or liposomes as described in the following sections.

1,2-dipalmitoyl-*sn*-glycero-3-phosphocholine (DPPC), 1,2-dimyristoyl-*sn*-glycero-3-phospho-(1'-rac-glycerol) (DMPG) and 1,2-distearoyl-*sn*-glycero-3- phosphoethanolamine-N-[methoxy(polyethylene glycol)-3000] (*m*-PEG_{3000}-DSPE) were purchased from Avanti Polar Lipids (Birminghan, AL). 3-[4,5-dimethylthiazol-2-yl]-2,5-diphenyltetrazolium bromide (MTT) and Cremophor EL were purchased from Sigma-Aldrich Chemical Co. (St. Louis, MO). MicroBCA protein assay kit was purchased from Pierce Protein Research Products (Rockford, IL) and used according to the product information sheet. All other chemicals were commercially available reagents of at least analytical grade.

Micelle preparation

Cremophor micellar solution was prepared by mixing 1 mg of temocene with 2.5 mL of Cremophor EL solution (100 mg/mL) in dry tetrahydrofuran (THF); 1 mL of THF was added to this mixture. The final Cremophor/temocene ratio was 250:1 (w/w). The resulting solution was stirred until it became one phase and isotropic. The solvent was removed by rotary evaporation. The resulting dry film was completely dissolved in 3 mL of sterile 5% dextrose solution. The micellar suspension was filtered through 0.22 μm mixed cellulose ester filter under sterile conditions to remove unloaded temocene. The encapsulation efficiency was then determined by the ratio of temocene absorbance before and after filtration. The average size, polydispersity, and zeta potential of the micelles were determined by photon correlation spectroscopy (PCS). A Zetasizer Nano-ZS (Malvern Instruments, UK) and a 4 mW He-Ne laser (Spectra Physics), at an excitation wavelength of 633 nm, were used.

Liposome preparation and characterization

Temocene liposomes were prepared by microemulsification following standard procedures [23,24]. Briefly, DPPC/DMPG/PEG_{3000}-DSPE (67.5:7.5:1 molar ratio) mixture containing the porphycene at 75:1 lipid/photosensitizer molar ratio was evaporated to dryness from a dry tetrahydrofuran solution and kept in a vacuum desiccator overnight. Multilamellar vesicles (MLV) were prepared by hydration of the dried lipid films by vortexing for 30 min (alternating 30 s periods of heating and 30 s of vortexing) at a concentration of 10 mg lipid/mL in 10 mM phosphate buffer (pH 7.4) at 60 °C. The MLV dispersion was frozen and thawed (five times), sonicated (bath sonicator, 15 min, 60 °C) and microemulsified (EmulsiFlex B3 device, Avestin, Ottawa, Canada). Control liposomes were prepared in the same way but without the PS.

To enhance stability during storage, liposomes were lyophilized using 5% trehalose as cryoprotectant agent. 2 mL of liposomal suspension were placed in 4 mL glass vials and frozen at −80 °C (liquid nitrogen) during 3–5 hours. Vials were subsequently dried during 24 h at −55 °C and 0.04 mbar (Freeze Dryer Alpha 1-2/LD, Martin Christ GmbH, Germany). Lyophilized liposomes were rehydrated immediately before the experiments by adding 2 mL of sterile water. The resulting suspension was prewarmed at 60 °C during 15

min and vortexed for 30 min (alternating 30 s periods of heating/vortexing). The PS and the lipid content in the liposomes were evaluated before and after lyophilization/rehydration following standard procedures. Liposomes were disrupted by the addition of DMSO to an aliquot of the liposomal suspension, free of non-entrapped PS, and the absorbance was measured at λ_{max} of the Soret band. Lipid content was quantified by a colorimetric assay with ammonium ferrothiocyanate according to the method of Stewart [25]. The average size, polydispersity, and zeta potential of the unilamellar vesicles were determined by PCS. Before measuring, samples were appropriately diluted to avoid multiple scattering.

Cell lines

We used both the DBA/2 mastocytoma cell line P815 (ATCC, TIB-64) [26] and the BALB/c colon adenocarcinoma cell line CT26.CL25 (ATCC, CRL-2639) that expressed a tumor antigen, β-galactosidase [27]. Cell lines were cultured in Roswell Park Memorial Institute (RPMI) medium with L-glutamine and $NaHCO_3$ supplemented with 10% heat inactivated fetal bovine serum, penicillin (100U/mL) and streptomycin (100 μg/mL) (all from Sigma) at 37 °C in 5% CO_2 in 75 cm^2 flasks (Falcon, Invitrogen). CT26.CL25 cells were cultured in constant presence of 500 μg/mL G418 antibiotic in order to maintain constant expression of the β-galactosidase.

Light source

A Lumacare lamp (Newport Beach, CA) fitted with a light guide and a 640–680 nm band-pass filter was used. Light guides were adjusted to give a uniform spot with an irradiance of 20 mW/cm^2 for *in vitro* experiments, and 100 mW/cm^2 for *in vivo* treatments. Light power was measured with a power meter (model DMM 199 with 201 standard head, Coherent, Santa Clara, CA).

In vitro PDT studies

P815 cells (5,000 cells/well) were plated in flat-bottom 96-well plates (Fisher Scientific, Pittsburgh, PA). Cells were allowed to attach for 24–48 h. They were then incubated in the dark with complete RPMI medium containing 0.1–10 μM temocene administered in the three different formulations. After 18 h incubation, cells were washed three times with PBS, replenished with fresh medium and 3.5 J/cm^2 of illumination were delivered at a fluence rate of 20 mW/cm^2. For time course incubation studies the different formulations were incubated with P815 cells at 1 μM temocene concentration for various times ranging from 2 to 24 h. Cells were then washed three times with PBS, replenished with fresh medium and subjected to 10 J/cm^2 PDT treatments. Irradiated cells were then incubated for 24 h and the MTT assay for cell viability was carried out [28]. Briefly, after washing with PBS, RPMI containing 0.05 mg/mL MTT was added and incubated for 4 h at 37 °C. The medium was replaced by DMSO and the absorbance at 550 nm was read on a Spectra Max 340 PC (Molecular Devices, Sunnyvale, CA) microplate reader. Each experiment was repeated three times.

Uptake studies

Cells were plated in 6-well plates and allowed to attach for 24–48 h. As described above, cells were incubated in the dark with complete RPMI medium containing 0.1–10 μM temocene administered in the three different formulations for 18 h. For time course uptake studies, cells were incubated with 1 μM temocene for times ranging from 2 to 24 h. Cells were then washed three times with PBS and disrupted with 0.5 mL of 2% sodium dodecyl sulfate (SDS) in Milli-Q water. The extent of PS uptake was assessed by comparison of the fluorescence of this cell lysate to that of standard solutions under the same conditions. The fluorescence intensity values obtained for each sample were normalized to the number of

cells determined by the bicinchoninic acid (BCA) protein assay [29]. Each experiment was repeated twice.

Subcellular localization

Cells were plated in clear flat-bottom 96-well plates and allowed to attach overnight. 1 μM temocene encapsulated in the three different formulations was added and incubated for 18 h. Cells were washed in PBS, and 5 μg/mL of (i) LysoTracker green DND-26, (ii) MitoTracker green FM, or (iii) ER-Tracker green (all from Molecular Probes Invitrogen) were added and incubated for 30 min at 37 °C. Cells were again washed in PBS and 5–10 min later a Olympus FV1000, multi-photon confocal microscope was used to image the cells. Quantification of overlap between organelle probes and the temocene localization were carried out using image processing and analysis (IPA) software from the public domain (ImageJ 1.42; http://rsbweb.nih.gov/ij/index.html) [30].

Animal tumor models

DBA/2 and BALB/c mice (6–8 weeks old) were purchased from Charles River Laboratories (Boston, MA). All experiments were carried out according to a protocol approved by the Subcommittee on Research Animal Care at (Institutional Animal Care and Use Committee) at Massachusetts General Hospital and were in accord with guidelines from the National Institutes of Health (NIH). Mice were inoculated with 350,000 cells subcutaneously into the depilated left thigh. Two orthogonal dimensions (a and b) of the tumor were measured 3–4 times a week with a vernier caliper. Tumor volumes were calculated as $4\pi/3\ [(a+b)/4]^3$. PDT was performed when tumors reached a diameter of 5–7 mm (around 9 days after cell inoculation).

PDT and tumor response

Tumor bearing mice were anaesthetized with an intraperitoneal injection of 87.5 mg/kg of ketamine and 12.5 mg/kg xylazine. Temocene (1 mg/kg) formulated in PEG/EtOH solution, Cremophor micelles or liposomes was administrated intravenously via the tail vein injection. 15 min or 24 h after injection of PS, 660-nm light (Lumacare) was used to irradiate a homogeneous spot of 1.5 cm diameter that covered the tumor and a margin of normal tissue. A total fluence of 75 or 150 J/cm^2 was delivered at a fluence rate of 100 mW/cm^2. The mice were sacrificed when any of the tumor diameters exceeded 1.5 cm or when any signs of disseminated metastatic tumor appeared (e.g., >15% loss of body weight).

In vivo fluorescence imaging

Tumor bearing mice were anaesthetized and subsequently placed in the light-tight chamber of the CRI Maestro (Caliper Life Sciences, Hopkinton, MA) *in vivo* fluorescence imaging system [31]. The instrument was set up as follows: images were captured every 10 nm throughout the wavelength range 650–800 nm using a 488-nm excitation filter, an LP 515-nm emission filter, and an exposure time of 100 ms. The focus and the stage height were set manually. Mice were imaged at different time points after temocene tail vein injection. After the fluorescence image acquisition, the image cubes were unmixed (deconvolved) using a spectral library containing the autofluorescence of the mice skin and a dilute sample of temocene in the different vehicles.

Statistics

Unpaired Student's *t* test was used to test for the significance level between two sets of measurements and Kaplan-Meier survival curves were compared with a log-rank test using GraphPad Prism version 5.00 for Windows, GraphPad Software, San Diego, CA www.graphpad.com. The level of significance was set to $p < 0.05$.

Results

Characterization of formulations

In order to compare the effect of the drug delivery system on PDT efficacy, temocene was dissolved in PEG_{400}/EtOH (3:2) or formulated in micelles or liposomes. The absorption spectra of temocene in the different delivery systems are shown in Fig. 1B. Dilution in water caused aggregation of temocene dissolved in PEG_{400}/EtOH mixture. Temocene incorporated in Cremophor EL micelles did not show spectral differences compared to THF, so it can be safely assumed that it is in a monomeric state. The incorporation of temocene into liposomes produced slight changes in its absorption spectrum, namely an intensity decrease of the Soret and Q bands. Similar changes have been observed previously for other PS in liposomes and have been attributed to the ordered lipid environment [24,32].

Table 1 summarizes the main features of the different formulations. The encapsulation efficiency of both liposomal and micellar formulation was higher than 90%. However, differences were found regarding the size and the zeta potential. PCS revealed a dynamic diameter of 30 ± 5 nm for micelles, whereas for liposomes it was 150 ± 20 nm. Likewise, the electric potential of the particles surface also differed between the formulations. Specifically, liposomes had a ζ_{pot} of −47 ± 2 mV, due to the phosphatidyl group of DMPG, which gives electrical stability to the colloid formulation. By contrast, Cremophor micelles had a ζ_{pot} close to zero. Despite this fact, the micellar formulation remained stable for several weeks and no flocculation or aggregation phenomena was observed. In this case, the thermodynamic stability came from the steric repulsive forces of the polymer-covered surface. No significant changes in the physicochemical properties were observed after lyophilization/rehydration of liposomes.

Effect of temocene formulation on PDT effectiveness *in vitro*

Studies of the effectiveness of the different temocene formulations are summarized in Fig. 2. P815 cells were incubated in the dark with different concentrations of temocene in the three formulations, exposed to red light, and assayed for cell survival. In the in vitro experiments, cells were incubated with different concentrations of temocene during 18 h. There was no dark toxicity in case of liposomal formulation at any of the concentrations tested, whereas the PEG/EtOH solutions showed substantial dark toxicity at high concentrations (Fig. 2A). In the presence of light, both formulations showed PDT-induced loss of mitochondrial activity in a concentration-, light dose- and incubation time-dependent manner (Fig. 2B, 2C and 2D), the PEG/EtOH solution being the most effective at the same concentration and light dose. Interestingly, no PDT effect could be observed with micelles, which showed the same extent of cell kill in the dark as upon delivery of a 3.5 or 10 J/cm^2 light dose. These results are consistent with the uptake studies (Fig. 2E) since minimal internalization was observed with the micellar formulation. Specifically, temocene internalization at 24 h was minimum for micelles, maximum for PEG/EtOH, and liposomes showing an intermediate behavior. Notwithstanding the lower uptake, it is worth noting that liposomes are the most effective vehicle when the photodynamic activity is compared on a per-molecule-cell uptake basis (Fig. 2F).

Subcellular localization

Confocal microscopy was used to examine the intracellular localization of temocene taken up after delivery by the different systems. For these studies the formulations were co-incubated with green-fluorescent probes specific for mitochondria (MitoTracker), lysosomes (LysoTracker) and endoplasmic reticulum (ER-Tracker). The overlaid images and the fluorescent topographic profiles are shown in Fig. 3. The stained patterns of the mitochondrial probe and temocene were different regardless of the formulation, indicating

marginal accumulation of the PS in the mitochondria. The fluorescent profile of temocene perfectly matched with the green fluorescence of the lysosomal probe for all formulations. In the case of ER probe, the overlapping was partial. It is important to note that it was necessary to use a higher exposure time for the micrographs of cells incubated with Cremophor micelles due to the limited internalization. No morphological changes were detected in the cells under these conditions and no relocalization of the PS was observed when cells were exposed to confocal excitation light.

Effect of temocene formulation on tumor accumulation *in vivo*

Temocene incorporated in PEG/EtOH, micelles or liposomes was injected intravenously through the tail vein in a dose of 1 mg/kg in tumor bearing mice. Temocene dissolved in PEG/EtOH induced death of all mice immediately after injection because of aggregation of PS in the blood stream that provoked the collapse of lungs and kidneys (see Supplementary data for histology studies). We checked that this toxicity was not due to PEG/EtOH mixture alone (no temocene). The PEG/EtOH formulation was consequently discarded for *in vivo* experiments. The tumor accumulation of temocene incorporated in micelles or liposomes was studied by non-invasive methods using a Maestro *in vivo* fluorescence camera system. Non-invasive fluorescence imaging provides a fast and convenient method to qualitatively compare the photosensitizer tumor accumulation profile when it is administered in different vehicles. Since the fluorescence quantum yield of temocene is different in liposomes and in micelles (data not shown), the fluorescence intensity of temocene could not be strictly comparable and only the tumor accumulation profile as function of time after i.v. administration was analyzed. The results are shown in Fig. 4. The pharmacokinetics of tumor uptake was influenced by the drug delivery system. Liposomal temocene showed a maximum in fluorescence intensity 24 h after injection. In the case of the micellar formulation, the fluorescence reached its highest intensity 8 h after injection. A high tumor-to-normal tissue ratio for a PS is considered to be important in PDT to ensure the maximum selectivity of the treatment and minimal normal tissue damage. Liposomes showed a better tumor selectivity, accumulating in the tumor three-times higher than in the surrounding skin. It is important to note that no significant effect on tumor growth was observed after drug injection (no light, dark control) as compared to absolute control mice (no light and no drug).

Effect of temocene formulation and targeting strategy on PDT effectiveness *in vivo*

Tumor bearing mice were divided into the following groups and each group included 8–10 animals: (i) control groups: dark control (no light), light control (no drug), absolute control (no light and no drug); (ii) vascular response group: mice treated with 150 J/cm^2 15 min after i.v. injection of 1 mg/kg liposomal or micellar temocene; (iii) cellular response group: mice treated with 150 J/cm^2 24 h after i.v. injection of 1 mg/kg liposomal or micellar temocene.

Mean tumor volumes plot and Kaplan-Meier survival analysis are shown in Fig. 5. In all cases, PDT produced a local response in P815-treated tumors, as manifested by an acute inflammation and edema in the first 24 h after treatment followed by tumor necrosis and a dark eschar formation over the area formerly occupied by the tumor. Subsequently a marked reduction in tumor size was observed. Animals were observed for up to 60 days after treatment for metastasis development, tumor regrowth and tissue healing. No significant differences in survival or tumor volume progress were observed between the different control groups so we only plotted absolute controls for the sake of clarity. The combined therapy of micellar formulation with short drug-to-light interval was clearly the most effective combination. This group resulted in a total regression of the principal tumor and stayed in remission for the whole course of observation (Fig. 5A). It is important to note that

although P815 grew as localized subcutaneous tumors, they also metastasized to draining lymph nodes and liver fairly early in the course of disease (Supplementary Fig. S3E–F) so the complete regression of principal tumor does not consequently imply the animal survival. In this case, temocene encapsulated in micelles resulted in a delay or even avoidance (3 out of 8 mice) of mice death (Fig. 5C). The vascular PDT regime using the liposomal formulation of temocene was not highly effective resulting in a local tumor regrowth relatively quickly. In marked contrast was the cellular targeting strategy (Fig. 5B and 5D). Liposomal treatment led to a delay of tumor regrowth and a significant survival advantage. PDT performed 24 hours after injection of temocene in Cremophor micelles had no effect in terms of survival compared to controls and local tumor regrew few days after treatment.

Treatments were also tested in a BALB/c mouse tumor model. CT26.CL25 tumor cells were inoculated subcutaneously in the left thigh and the same treatments were performed, namely 1 mg/kg temocene in micellar or liposomal formulation, and 150 J/cm^2 of light dose at 15 min or 24 h after injection. Under these conditions, all treatments worked perfectly resulting in a total tumor regression 4 days after PDT performance. Only when the light dose was reduced to 75 J/cm^2 (Supplementary Fig. S4) we obtained a differential response. Liposomes in a short drug-to-light interval were not effective and the tumor volume evolution was similar to control group.

Discussion

The mechanisms of action for PDT are complex, depending upon the PS, light dosimetry, drug delivery system, and treatment conditions. Temocene (*m*-tetrahydroxyphenyl porphycene) is a novel promising PS whose photophysical properties and *in vitro* PDT efficacy in DMSO were recently studied [22]. However, the inherent unsuitability of DMSO prompted us to consider formulating temocene in different drug delivery systems. The formulation of a PS plays an important role in its activity by modulating the pharmacokinetics, uptake, and subcellular distribution and localization. The present study investigated the effect of three different vehicles, namely PEG_{400}/EtOH solutions, Cremophor micelles, and DPPC/DMPG/PEG_{3000}-DSPE liposomes, on the PDT effectiveness of temocene.

Micelles, prepared by film formation and hydration just before experiments, and liposomes, prepared by microemulsification and then lyophilized to guarantee a long-term stability during all the experimental stage, allowed for a high encapsulation of temocene in a monomeric state. Aggregation of the PS was evident when delivered in PEG_{400}/EtOH solution. In spite of this fact, this formulation showed the best *in vitro* response because cells were able to internalize the largest amount of PS. However, the killing efficacy per uptaken molecule was higher in the case of liposomes. A minimal internalization and, therefore, no photocytotoxic effect were observed with the micellar formulation. Attempts to modify this situation by removing serum or diluting beyond the critical micellar concentration proved unsuccessful. No redistribution effects were observed in presence of serum indicating that temocene remained entrapped in micelles during cell incubation (Supplementary Fig. S1). A literature search revealed that in some circumstances intact micelles are hardly taken up by cells [33–35]. It should be noted that Cremophor EL would not be a suitable micellar formulation to be used for clinical applications. Cremophor EL is known to induce a pseudo-allergic reaction by activation of the complement system [36], even though the mice in this study showed no ill-effects of Cremophor EL micelle administration. Alternative micellar formulations such as poly(ε-caprolactone)-poly(ethylene glycol)-poly(ε-caprolactone) triblock copolymers [37] could be studied that would have less risk of toxicity.

Regarding the subcellular localization of temocene internalized in the different drug delivery systems, *in vitro* experiments performed with organelle-specific fluorescent probes revealed no difference between the vehicles. In all cases, lysosomes were the preferential site of temocene accumulation in P815 cells. These results differed from those obtained in a previous work in HeLa cells, where temocene preferentially localized in mitochondria [22]. However, in that work temocene had been delivered in DMSO, which is a membrane permeabilizer [38], whereas the drug delivery systems used in the current experiments internalize drugs mainly by endocytosis, which is characterized by the formation of endocytic vacuoles (lysosome progenitors) [39, 40].

Drug delivery systems can also modulate *in vivo* pharmacokinetics and tumor accumulation. P815 tumor bearing mice were studied by non-invasive methods at different times after i.v. injection of the different formulations. Although temocene in PEG/EtOH solution could be considered a promising formulation based on its good *in vitro* response, the formulation failed when it was administered intravenously causing the immediate death of the mice due to aggregation of the PS in the blood stream. *In vivo* fluorescence imaging studies demonstrated that there was no specific tumor accumulation of temocene after 15 min. On the other hand, the kinetics of tumor uptake with the liposomal formulation showed the highest tumor extravasation 24 h after injection. Micelles showed a faster tumor accumulation that can be explained by the rapid clearance of micelles by reticuloendothelial system. Pegylated liposomes exhibit steric stabilization and avoid reticuloendothelial system uptake, resulting in prolonged circulation times and enhanced selective localization. The accumulation of macromolecules in tumors is mainly due to the so-called enhanced permeability and retention effect and this progressive phenomenon can be greatly favored by prolonging the half-life in plasma of nanoparticles [20,41,42]. This effect is also dependent of the size of nanoparticles: small carriers can diffuse in and out of the tumor blood vessels because of their small size, and, hence, the effective concentration of the drug in the tumor diminishes compared to larger vehicles [43]. Thus, the difference of size between temocene loaded micelles (30 nm) and liposomes (180 nm) can also affect the kinetics of drug accumulation in the tumor. Liposomes also showed the best tumor selectivity, namely a tumor-to-normal-tissue ratio of 3.

The time between PS administration and light treatment is also a critical parameter for PDT efficiency. The best PDT response was obtained when light irradiation was delivered 15 min after micelle-loaded temocene injection. This treatment led to an acute inflammatory reaction as evidenced by a large amount of edema in the treated leg, which resulted in total regression of the primary tumor with extended survival. Vascular perfusion results also demonstrate that the major target for the 15 min interval micellar PDT treatment is tumor vasculature causing the disruption of functional blood vessels (Supplementary Fig. S5). In a cellular-targeted regimen, liposomal temocene exhibited the best PDT response. Tumor regrowth was delayed, although not fully prevented, and mouse survival was improved. In this case, micelles were not effective. These results agree with the 3-fold higher tumor accumulation of the PS attained by liposomes relative to Cremophor micelles.

These results were also corroborated using the BALB/c mouse model tumor. Delivery of the same light and drug doses used in the P815 tumor experiments (150 J/cm^2, 1 mg/kg temocene) caused a total regression of tumor in all cases. Only when the light dose was halved (75 J/cm^2), the vascular response of liposomal formulation had no effect in terms of tumor volume diminution and the advantage of the micellar formulation could be appreciated (Supplementary Fig. S4).

To summarize our findings, we have confirmed that both the drug delivery system chosen and the targeting strategy employed can determine the PDT effectiveness of the new PS

temocene both *in vitro* and *in vivo.* It is important to mention that *in vitro* tests not always reproduce *in vivo* results. Micelles showed no PDT activity in cell cultures while they were the most effective formulation for *in vivo* PDT treatments combined with a short drug-to-light interval. This of course reflects that this formulation targets the tumor vasculature, which *in vitro* cultures lack. In contrast, temocene in PEG/EtOH solutions could have been regarded as a good vehicle based on the *in vitro* results but caused immediate toxicity when they were administered intravenously. Liposomes are the best vehicle in terms of achieving cell internalization and tumor selectivity. In conclusion, we have shown that PDT with the novel PS temocene has significant therapeutic effects in a metastatic tumor model, both for a vascular-targeted treatment with its Cremophor EL formulation, and also for a cellular strategy when it is encapsulated in DPPC/DMPG/PEG_{3000}-DSPE liposomes.

Supplementary Material

Refer to Web version on PubMed Central for supplementary material.

Acknowledgments

This work was supported by grants of the Spanish Ministry of Economy and Competitiveness (CTQ2010-20870-C03) and US NIH (RO1 AI050875) to MR Hamblin. M G-D thanks the Comissionat per a Universitats i Recerca del Departament d'Innovació, Universitats i Empresa de la Generalitat de Catalunya i del Fons Social Europeu for a predoctoral fellowship. The sponsors had no influence on the collection, analysis and interpretation of data; on the writing of the report; and on the decision to submit the article for publication. We thank Dr. David Sánchez-García for the synthesis of temocene and Dr. Salvador Borrós for the assistance with the Zetasizer Nano-ZS measurements.

Abbreviations

BCA	bicinchoninic acid
DMEM	Dulbecco´s Modified Eagle´s Medium
DMPG	1,2-dimyristoyl-*sn*-glycero-3-phospho-(1'-rac-glycerol)
DMSO	dimethyl sulfoxide
DPPC	1,2-dipalmitoyl-*sn*-glycero-3-phosphocholine
***m*-PEG_{3000}-DSPE**	1,2-distearoyl-*sn*-glycero-3-phosphoethanolamine-N-[methoxy(polyethylene glycol)-3000]
FBS	fetal bovine serum
MLV	multilamellar vesicle
MTT	3-[4,5-dimethylthiazol-2-yl]-2,5-diphenyltetrazolium bromide
PBS	phosphate buffered saline
PCS	photon correlated spectroscopy
PEG	polyethylene glycol
PDT	photodynamic therapy
PS	photosensitizer
ROS	reactive oxygen species
RPMI	Roswell Park Memorial Institute
SDS	sodium dodecyl sulfate
THF	tetrahydrofuran

References

1. Agostinis P, Berg K, Cengel KA, Foster TH, Girotti AW, Gollnick SO, Hahn SM, Hamblin MR, Juzeniene A, Kessel D, Korbelik M, Moan J, Mroz P, Nowis D, Piette J, Wilson BC, Golab J. Photodynamic therapy of cancer: An update. CA Cancer J. Clin. 2011; 61:250–281. [PubMed: 21617154]
2. Dougherty TJ, Gomer CJ, Henderson BW, Jori G, Kessel D, Korbelik M, Moan J, Peng Q. Photodynamic therapy. J. Natl. Cancer Inst. 1998; 90:889–905. [PubMed: 9637138]
3. Castano AP, Demidova TN, Hamblin MR. Mechanisms in photodynamic therapy: part two: cellular signaling, cell metabolism and modes of cell death. Photodiagnosis Photodyn. Ther. 2005; 2:1–23.
4. Robertson CA, Evans DH, Abrahamse H. Photodynamic therapy (PDT): a short review on cellular mechanisms and cancer research applications for PDT. J. Photochem. Photobiol. B: Biol. 2009; 96:1–8.
5. Dewaele M, Verfaillie T, Martinet W, Agostinis P. Death and survival signals in photodynamic therapy. Methods Mol. Biol. 2010; 635:7–33. [PubMed: 20552337]
6. Dolmans DEJGJ, Fukumura D, Jain RK. Photodynamic therapy for cancer. Nat. Rev. Cancer. 2003; 3:380–387. [PubMed: 12724736]
7. Krammer B. Vascular effects of photodynamic therapy. Anticancer Res. 2001; 21:4271–4277. [PubMed: 11908681]
8. Preise D, Scherz A, Salomon Y. Antitumor immunity promoted by vascular occluding therapy: lessons from vascular-targeted photodynamic therapy (VTP) . Photochem. Photobiol. Sci. 2011; 10:681–688. [PubMed: 21258718]
9. Chen B, Pogue BW, Luna JM, Hardman RL, Hoopes PJ, Hasan T. Tumor vascular permeabilization by vascular-targeting photosensitization: effects, mechanism, and therapeutic implications. Clin. Cancer Res. 2006; 12:917–923. [PubMed: 16467106]
10. St Denis TG, Aziz K, Waheed AA, Huang YY, Sharma SK, Mroz P, Hamblin MR. Combination approaches to potentiate immune response after photodynamic therapy for cancer. Photochem. Photobiol. Sci. 2011; 10:792–801. [PubMed: 21479313]
11. Korbelik M. Cancer vaccines generated by photodynamic therapy. Photochem. Photobiol. Sci. 2011; 10:664–669. [PubMed: 21258728]
12. Mroz P, Hashmi JT, Huang YY, Lange N, Hamblin MR. Stimulation of antitumor immunity by photodynamic therapy. Expert Rev. Clin. Immunol. 2011; 7:75–91. [PubMed: 21162652]
13. Madar-Balakirski N, Tempel-Brami C, Kalchenko V, Brenner O, Varon D, Scherz A, Salomon Y. Permanent occlusion of feeding arteries and draining veins in solid mouse tumors by vascular targeted photodynamic therapy (VTP) with Tookad. PLoS One. 2010; 5:e10282. [PubMed: 20421983]
14. Brown SB, Mellish KJ. Verteporfin: a milestone in opthalmology and photodynamic therapy. Expert Opin. Pharmacother. 2001; 2:351–361. [PubMed: 11336591]
15. Chevalier S, Anidjar M, Scarlata E, Hamel L, Scherz A, Ficheux H, Borenstein N, Fiette L, Elhiali M. Preclinical study of the novel vascular occluding agent, WST11, for photodynamic therapy of the canine prostate. J. Urol. 2011; 186:302–309. [PubMed: 21600602]
16. Weersink RA, Bogaards A, Gertner M, Davidson SR, Zhang K, Netchev G, Trachtenberg J, Wilson BC. Techniques for delivery and monitoring of TOOKAD (WST09)-mediated photodynamic therapy of the prostate: clinical experience and practicalities. J. Photochem. Photobiol. B. 2005; 79:211–222. [PubMed: 15896648]
17. Moore CM, Pendse D, Emberton M. Photodynamic therapy for prostate cancer-- a review of current status and future promise. Nat. Clin. Pract. Urol. 2009; 6:18–30. [PubMed: 19132003]
18. Bechet D, Couleaud P, Frochot C, Viriot ML, Guillemin F, Barberi-Heyob. Nanoparticles as vehicles for delivery of photodynamic therapy agents M. Trends Biotechnol. 2008; 26:612–621. [PubMed: 18804298]
19. Li WT. Nanotechology-based strategies to enhance the efficacy of photodynamic therapy for cancers. Curr. Drug Metab. 2009; 10:851–860. [PubMed: 20214580]
20. Konan YN, Gurny R, Allemann E. State of the art in the delivery of photosensitizers for photodynamic therapy. J. Photochem. Photobiol. B. 2002; 66:89–106. [PubMed: 11897509]

21. Reddi E. Role of delivery vehicles for photosensitizers in the photodynamic therapy of tumours. J. Photochem. Photobiol. B. 1997; 37:189–195. [PubMed: 9085566]
22. García-Díaz M, Sánchez-García D, Soriano J, Sagristà ML, Mora M, Villanueva á, Stockert JC, Cañete M, Nonell S. Temocene: the porphycene analogue of temoporfin (Foscan®). Med. Chem. Commun. 2011; 2:616–619.
23. García-Díaz M, Nonell S, Villanueva á, Stockert JC, Cañete M, Casadò A, Mora M, Sagristà ML. Do folate-receptor targeted liposomal photosensitizers enhance photodynamic therapy selectivity? . Biochim. Biophys. Acta. 2011; 1808:1063–1071. [PubMed: 21215723]
24. Postigo F, Sagristà ML, De Madariaga MA, Nonell S, Mora M. Photosensitization of skin fibroblasts and HeLa cells by three chlorin derivatives: Role of chemical structure and delivery vehicle. Biochim. Biophys. Acta. 2006; 1758:583–596. [PubMed: 16740249]
25. Stewart JC. Colorimetric determination of phospholipids with ammonium ferrothiocyanate. Anal. Biochem. 1980; 104:10–14. [PubMed: 6892980]
26. Van den Eynde B, Lethe B, Van Pel A, De Plaen E, Boon T. The gene coding for a major tumor rejection antigen of tumor P815 is identical to the normal gene of syngeneic DBA/2 mice. J. Exp. Med. 1991; 173:1373–1384. [PubMed: 1903428]
27. Wang M, Bronte V, Chen PW, Gritz L, Panicali D, Rosenberg SA, Restifo NP. Active immunotherapy of cancer with a nonreplicating recombinant fowlpox virus encoding a model tumor-associated antigen. J. Immunol. 1995; 154:4685–4692. [PubMed: 7722321]
28. Mosmann T. Rapid Colorimetric Assay for Cellular Growth and Survival - Application to Proliferation and Cyto-Toxicity Assays. J. Immunol. Methods. 1983; 65:55–63. [PubMed: 6606682]
29. Smith PK, Krohn RI, Hermanson GT, Mallia AK, Gartner FH, Provenzano MD, Fujimoto EK, Goeke NM, Olson BJ, Klenk DC. Measurement of protein using bicinchoninic acid. Anal. Biochem. 1985; 150:76–85. [PubMed: 3843705]
30. Alvarez M, Villanueva A, Acedo P, Canete M, Stockert JC. Cell death causes relocalization of photosensitizing fluorescent probes. Acta Histochem. 2011; 113:363–368. [PubMed: 20138336]
31. Mroz P, Huang YY, Szokalska A, Zhiyentayev T, Janjua S, Nifli AP, Sherwood ME, Ruzie C, Borbas KE, Fan D, Krayer M, Balasubramian T, Yang E, Kee HL, Kirmaier C, Diers JR, Bocian DF, Holten D, Lindsey JS, Hamblin MR. Stable synthetic bacteriochlorins overcome the resistance of melanoma to photodynamic therapy. FASEB J. 2010; 24:3160–3170. [PubMed: 20385618]
32. Postigo F, Mora M, De Madariaga MA, Nonell S, Sagristà ML. Incorporation of hydrophobic porphyrins into liposomes: characterization and structural requirements. Int. J. Pharm. 2004; 278:239–254. [PubMed: 15196629]
33. Hofman JW, Carstens MG, van Zeeland F, Helwig C, Flesch FM, Hennink WE, van Nostrum CF. Photocytotoxicity of mTHPC (temoporfin) loaded polymeric micelles mediated by lipase catalyzed degradation CF. Pharm. Res. 2008; 25:2065–2073. [PubMed: 18597164]
34. Kessel D. Properties of cremophor EL micelles probed by fluorescence. Photochem. Photobiol. 1992; 56:447–451. [PubMed: 1454875]
35. Woodburn K, Chang CK, Lee S, Henderson B, Kessel D. Biodistribution and PDT efficacy of a ketochlorin photosensitizer as a function of the delivery vehicle. Photochem. Photobiol. 1994; 60:154–159. [PubMed: 7938213]
36. Wang H, Wang HS, Liu ZP. Agents that induce pseudo-allergic reaction. Drug Discov. Ther. 2011; 5:211–219. [PubMed: 22466368]
37. Zhang L, He Y, Ma G, Song C, Sun H. Paclitaxel-loaded polymeric micelles based on poly(ε -caprolactone)-poly(ethylene glycol)-poly(ε-caprolactone) triblock copolymers: in vitro and in vivo evaluation. Nanomedicine. 2011
38. Notman R, Noro M, O'Malley B, Anwar J. Molecular basis for dimethylsulfoxide (DMSO) action on lipid membranes. J. Am. Chem. Soc. 2006; 128:13982–13983. [PubMed: 17061853]
39. Hillaireau H, Couvreur P. Nanocarriers' entry into the cell: relevance to drug delivery. Cell Mol.Life Sci. 2009; 66:2873–2896. [PubMed: 19499185]
42. Conner SD, Schmid SL. Regulated portals of entry into the cell. Nature. 2003; 422:37–44. [PubMed: 12621426]

40. Iyer AK, Khaled G, Fang J, Maeda H. Exploiting the enhanced permeability and retention effect for tumor targeting. Drug Discov. Today. 2006; 11:812–818. [PubMed: 16935749]

42. Fang J, Nakamura H, Maeda H. The EPR effect: Unique features of tumor blood vessels for drug delivery, factors involved, and limitations and augmentation of the effect. Adv. Drug Deliv. Rev. 2011; 63:136–151. [PubMed: 20441782]

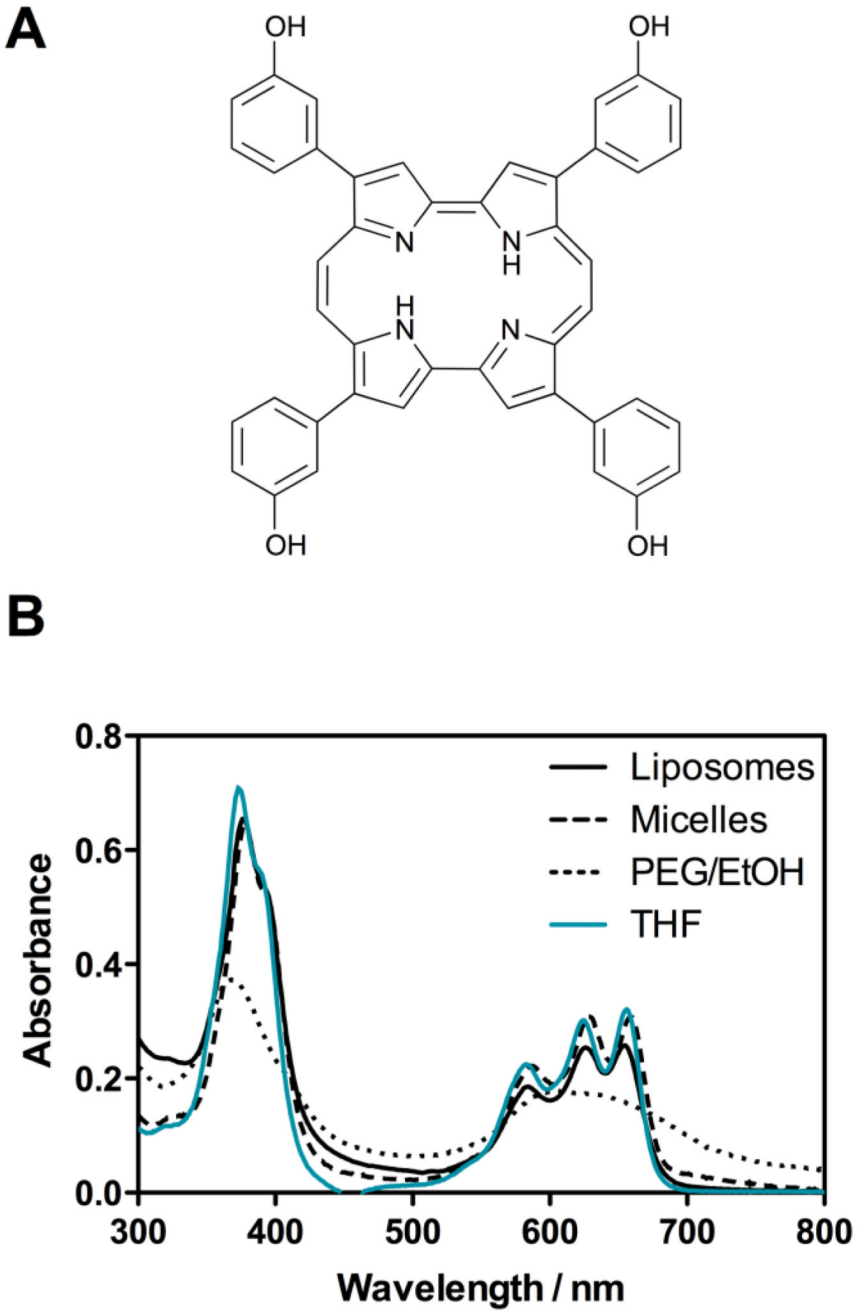

Fig. 1.

A) Chemical structure of temocene. B) Absorption of 2.5 μM temocene in aqueous suspensions of different drug delivery systems: liposomes (black solid line), micelles (dashed line), PEG/EtOH (dotted line). Absorption of temocene dissolved in THF (blue solid line) is shown for comparison.

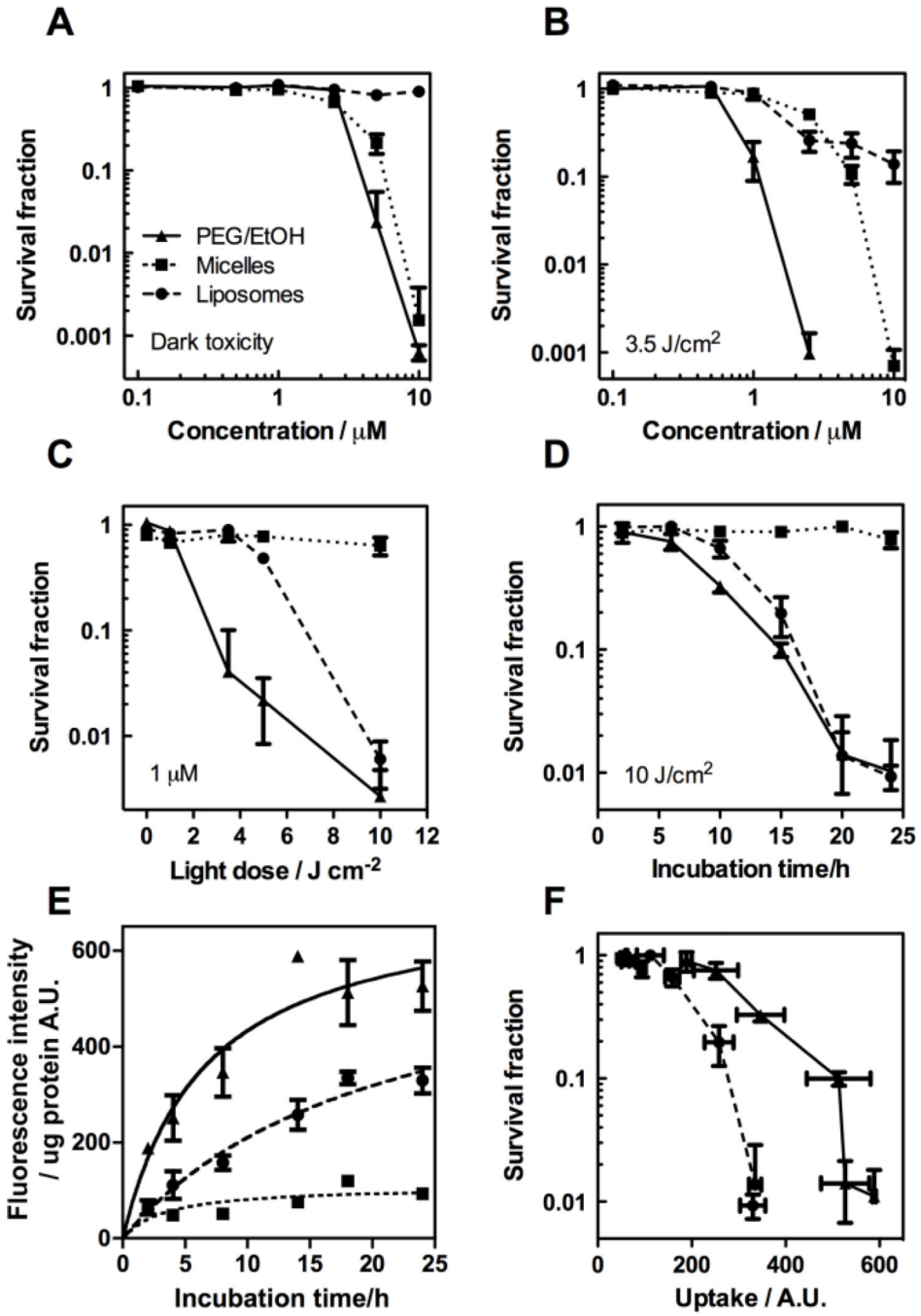

Fig. 2.

In vitro PDT effectiveness of temocene dissolved in PEG/EtOH (triangles) or encapsulated in micelles (squares) or liposomes (circles). A) Dark toxicity after 18 h incubation in P815 cell line. B) Effectiveness of 3.5 J/cm^2 after 18 h incubation. C) Light dose dependence after 18 h incubation. D) Effectiveness of 10 J/cm^2 after different incubation times. E) Cellular uptake by P815 cells. F). PDT effectiveness after 10 J/cm^2 per unit uptake.

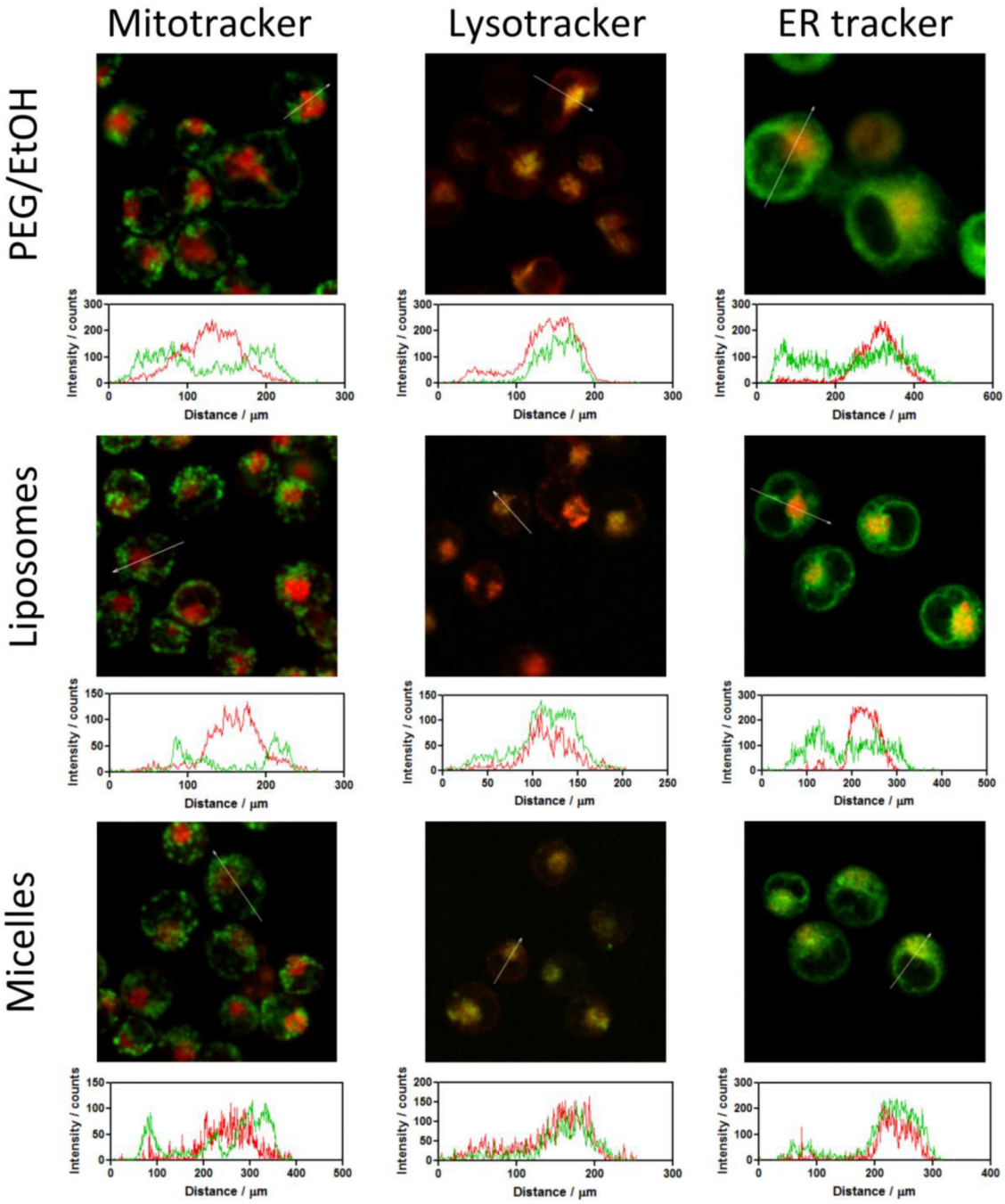

Fig. 3.

Fluorescence micrographs of P815 cells showing red fluorescence from temocene in different formulations overlaid with green fluorescence from lysotracker, mitotracker or ER-tracker. Fluorescent topographic profiles of cells are showed under confocal images. Arrow indicates the analyzed longitudinal transcellular zone.

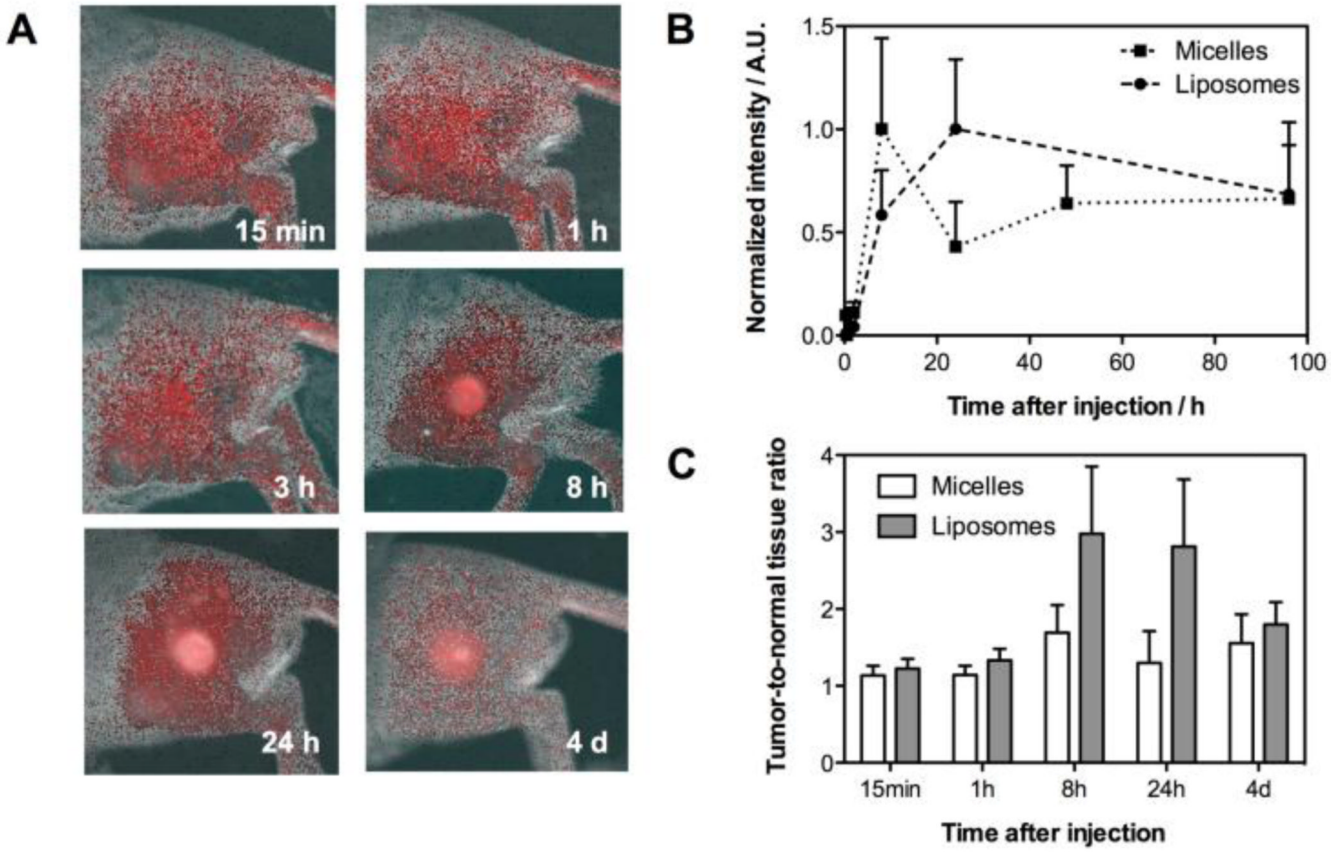

Fig. 4.

Tumor accumulation of temocene incorporated in micelles or liposomes after i.v. injection. A) Series of *in vivo* fluorescence images of temocene encapsulated in liposomes accumulated in P815 tumor. B) Fluorescence intensity of temocene in P815 tumor at different times after i.v. injection (the intensities have been normalized to facilitate comparison of their time profile). C) Tumor-to-normal tissue ratio calculated by the fraction of the fluorescence intensity in the tumor and the fluorescence intensity in the surrounding skin. Data show the mean ± SD of three mice.

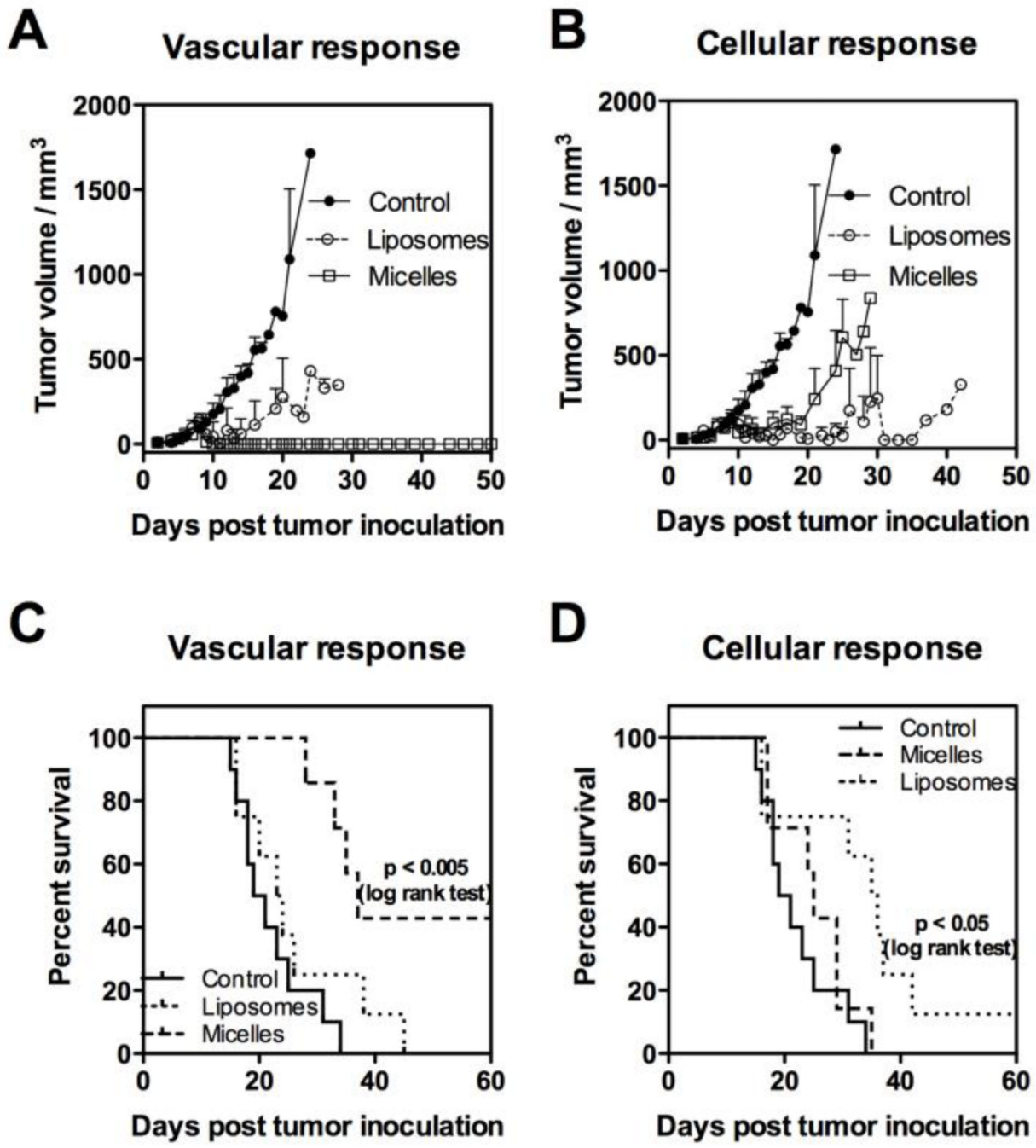

Fig. 5.

Panels A and B) Plots of mean tumor volumes in mice bearing P815 tumor. Points are means of 8–10 tumors and bars are SD. Panels C and D) Kaplan-Meier survival curves of % mice cured from P815 tumors. Vascular response: PDT performed 15 min after i.v. injection of 1 mg/kg formulated temocene. Cellular response: PDT performed 24 h after i.v. injection of 1 mg/kg formulated temocene. Light dose: 150 J/cm^2

Table 1

Physicochemical characteristics of the different formulations as measured by PS and lipid content, particle size and zeta potential.

Formulation	%PS[a]	%L[b]	Zave/nm[c]	ζpot/mV[d]
Micelles	95 ± 2	n.a.	30 ± 5	−1.5 ± 0.5
Liposomes	90 ± 3	85 ± 5	150 ± 20	−47 ± 2
Liposomes after lyophilization/rehydration	90 ± 5	90 ± 5	180 ± 20	−55 ± 5

Data are mean values ± SD of at least three independent experiments.

[a] %PS: Encapsulation efficiency expressed as the percentage of PS in the sample with respect to the PS present at the initial stage of preparation.

[b] %L: Lipid content, expressed as the percentage of lipid in the sample with respect to the lipid present at the initial stage of liposome preparation.

[c] Z average mean.

[d] Zeta potential.

n.a. not applicable